Thermal pressurization model in 3-D dynamic spontaneous rupture model with cohesive zone

Andrea Bizzarri, Massimo Cocco

Istituto Nazionale di Geofisica e Vulcanologia

Sezione di Sismologia e Tettonofisica

bizzarri@bo.ingv.it, cocco@ingv.it - http://www.ingv.it

Fall Meeting 2004

T23A-0572

Abstract

We simulate an earthquake rupture through a 3-D Finite Difference algorithm using the Traction-At-Split-Nodes Fault Boundary Condition. The dynamic rupture propagation is governed by an assigned constitutive law, which controls the breakdown processes within the cohesive zone. Seismic slip on faults produces temperature perturbations. Fault heating is controlled by the mechanical properties of the fault surface and by the rheological properties of the gouge layer. We model the temperature evolution on the fault through the heat flow equation and we couple these thermal variations with the fluid pressure changes by using the Darcy's law for fluid flow in porous media and the continuity equation of fluid mass in a solid. We assume that the increase of temperature does not change the adopted R&S constitutive parameters during the dynamic instability. To model the temporal variations of effective normal stress we consider a constant porosity within the slip zone and the evolution equation for the state variable proposed by Linker and Dieterich (1992, *JGR, 97*). Finally, we link this constitutive model with the evolution law for porosity proposed by Segall and Rice (1995, *JGR, 101*). The goal of this study is to investigate dynamic fault weakening caused by shear heating and thermal pressurization of pore fluids. We show how these phenomena may complicate the dynamic traction evolution and affect dynamic fault strength. Our simulations reveal that the effect of frictional heating and temperature increase strongly depend on the thickness of the slip zone. Thus, our 3-D simulations confirm that thermal pressurization is a viable mechanism to explain earthquake ruptures.

Frictional Heating on the Fault Surface

We solve the fundamental elasto-dynamic equation to model a fully 3-D spontaneous dynamic rupture on a planar fault surface by using a Finite Difference algorithm described in Bizzarri and Cocco (2004, *Ann. Geophys., in press*) with the Traction-at-Split-Nodes technique (Andrews, 1999, *BSSA, 89*). The dynamic rupture propagation is governed by an assumed constitutive law (the linear slip-weakening law – SW – or rate- and state-dependent – R&S – friction laws; see Panel A). The shear fault friction is $\tau = \mu\sigma_n^{eff}$, where σ_n^{eff} is the effective normal stress ($\sigma_n^{eff} = \sigma_n - p_{fluid}$). Fault slip produces temperature perturbations that can be described by the 1-D Fourier heat conduction equation. The heat source q (or the rate of frictional heat generation within the slipping zone) in a generic fault point (ξ_1,ξ_2) is calculated as (Cardwell et al., 1978, *GJRAS, 52, 525*; Fialko, 2004, *JGR, 109*):

$$q(\xi_1,\xi_2,\zeta,t)=\begin{cases}\dfrac{\tau(\xi_1,\xi_2,t)v(\xi_1,\xi_2,t)}{2w(\xi_1,\xi_2)} & ,t>0,|\zeta|\le w(\xi_1,\xi_2)\\ 0 & ,|\zeta|>w(\xi_1,\xi_2)\end{cases}$$

where ζ is the coordinate normal to the fault, v is the fault slip velocity and $2w$ is the thickness of the slipping zone. Assuming that the heat capacity per unit volume of the bulk composite c and the thermal diffusivity χ are homogeneous over the normal coordinate ζ, on the fault surface ($\zeta = 0$) the temperature T is:

$$T^{wf}(\xi_1,\xi_2,t)=T_0^{\ f}+\frac{1}{2cw(\xi_1,\xi_2)}\int_0^{t-\varepsilon}\mathrm{d}t'\ \mathrm{erf}\left(\frac{w(\xi_1,\xi_2)}{2\sqrt{\chi(t-t')}}\right)\tau(\xi_1,\xi_2,t')v(\xi_1,\xi_2,t')$$

where $T_0^{\ f}$ is the initial temperature distribution on the fault plane ($T_0^{\ f} = T(\xi_1,\xi_2,0,0)$), erf(.) is the error function and ε is an arbitrary small positive real number. In Figure 1 we plot the temperature evolution for Dry faults governed by SW for different values of the gouge layer thickness $2w$. Dots indicate the time steps at which the total slip is reached in the healing cases (slight curves) and the same value of slip in the crack like cases (intense curves).

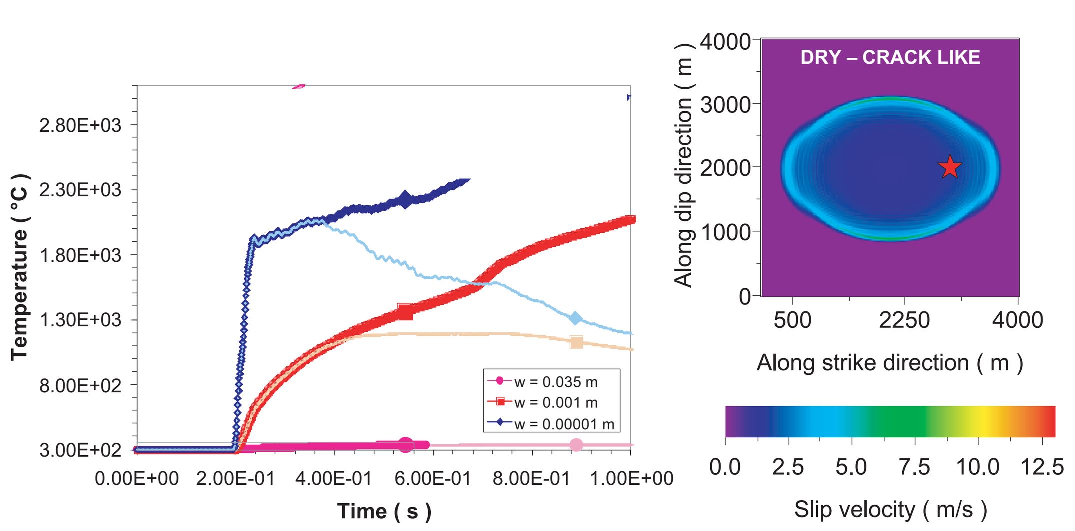

Figure 1

CONSTITUTIVE LAWS

SW law

$$\tau=\begin{cases}\tau_u-(\tau_u-\tau_f)\dfrac{u}{d_o} & u<d_o\\ \tau_f & u\ge d_o\end{cases}$$

DR – LD92 law

$$\tau=\left[\mu_*-a\ln\left(\frac{v_*}{v}+1\right)+b\ln\left(\frac{\Psi v_*}{L}+1\right)\right]\sigma_n^{eff}$$

$$\frac{\mathrm{d}}{\mathrm{d}t}\Psi=1-\frac{\Psi v}{L}-\left(\frac{\alpha_{DL}\Psi}{b\sigma_n^{eff}}\right)\frac{\mathrm{d}}{\mathrm{d}t}\sigma_n^{eff}$$

Panel A

Thermal Pressurization Model

We couple the thermal variations with the fluid pressure changes by using the Darcy' s law for fluid flow in porous media and the continuity of the fluid mass in a solid, assuming that: (*i*) the scale of the porosity is small compared with the other characteristic dimensions of the flow; and (*ii*) the flow in the individual channels is laminar (and therefore no advective terms are considered). Fluid pressure is related to the temperature caused by frictional heating (assuming that permeability k, cubic mass density ρ and dynamic viscosity η are independent on the position (i. e. spatially homogeneous)):

$$\frac{\partial}{\partial t}p_{fluid}-\frac{\alpha_{fluid}}{\beta_{fluid}}\frac{\partial}{\partial t}T+\frac{1}{\beta_{fluid}\phi}\frac{\partial}{\partial t}\phi=\omega\frac{\partial^2}{\partial\zeta^2}p_{fluid}$$

where α_{fluid} is the fluid expansivity, β_{fluid} is the fluid compressibility, Φ is the porosity and ω is the hydraulic diffusivity ($\omega = k/\eta\beta_{fluid}\Phi$). In the case of constant porosity ($\Phi(t) = \Phi_0$), in a generic fault point (ξ_1,ξ_2) and at a time t, the solution of this equation coupled with the heat conduction equations is:

$$p_{fluid}^{\ wf}(\xi_1,\xi_2,t)=p_{fluid_0}^{\ f}+\frac{\gamma}{2w(\xi_1,\xi_2)}\int_0^{t-\varepsilon}\mathrm{d}t'\left\{-\frac{\chi}{\omega-\chi}\mathrm{erf}\left(\frac{w(\xi_1,\xi_2)}{2\sqrt{\chi(t-t')}}\right)+\frac{\omega}{\omega-\chi}\mathrm{erf}\left(\frac{w(\xi_1,\xi_2)}{2\sqrt{\omega(t-t')}}\right)\right\}\tau(\xi_1,\xi_2,t')v(\xi_1,\xi_2,t')$$

where $\gamma = \alpha_{fluid}/(\beta_{fluid}c)$ and $p_{fluid_0}^{\ f}$ is the initial fluid distribution on the fault plane ($p_{fluid_0}^{\ f} = p_{fluid}(\xi_1,\xi_2,0,0)$). Figure 2 shows, for $w = 35$ mm, the temperature evolutions for a fault obeying to SW (top panels) and the superpositions of the solutions for crack like rupture with SW and R&S governing equations (bottom panels).

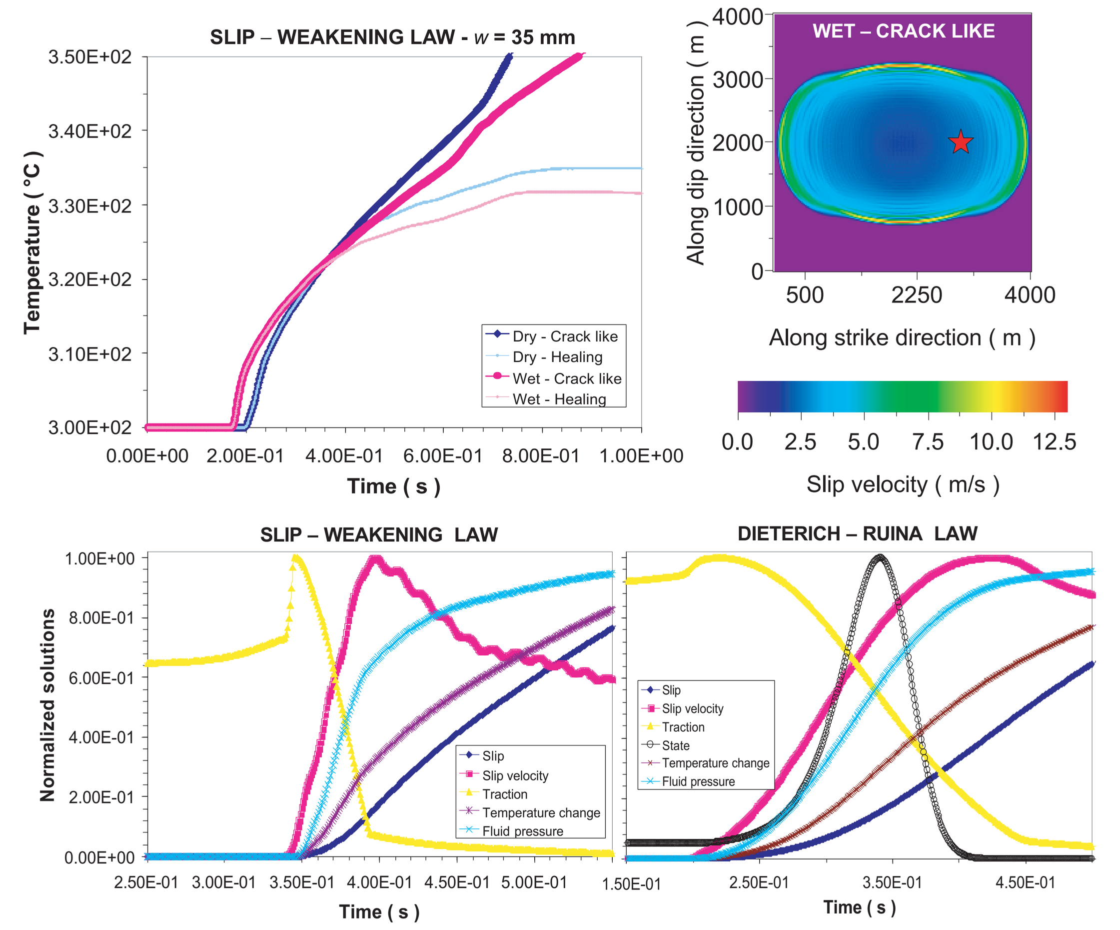

Figure 2

Parameter	Value
Medium and discretization parameters	
$\lambda = G$	27 GPa
v_P	5196 m/s
v_S	3000 m/s
$\sigma_n - p_{fluid_0}^{\ f}$	30 MPa
$\Delta x_1 = \Delta x_3$	25 m
Δx_2	100 m
Δt	0.83671×10^{-3} s
Slip-weakening model parameters	
τ_0	20 MPa
μ_u	0.93333
μ_f	0.33333
d_0	0.1 m
Rate– and state–dependent models parameters	
a	0.007
b	0.016
L	0.01 m
v_{init}	1×10^{-4} m/s
μ_*	0.56
α_{LD} (reference)	0.53
Thermal pressurization parameters	
α_{fluid}	1.5×10^{-3} °C^{-1}
β_{fluid}	1×10^{-9} Pa^{-1}
c	3×10^{6} J/(m^3 °C)
η	1×10^{-4} Pa s
k (reference)	5×10^{-17} m^2
χ	1×10^{-6} m^2/s
w (reference)	0.035 m
Φ	0.025

Table 1

List of the parameters adopted in numerical experiments.

Effects of Gouge Layer Thickness and Hydraulic Diffusivity

In all the numerical experiments presented in this work we assume for simplicity that the slip zone (or the gouge layer) thickness $2w$ is uniform over the whole fault surface. We show in Figure 3 the effects of the variable w (from 10 μm to 0.5 m) and of a variable hydraulic diffusivity ω (variable permeability over the range between 2.5e-20 and 1.e-15 m^2) on the solutions for a fault obeying SW law. In Figure 4 we have reported the same comparison for the R&S case. Blue curves represent the reference (Dry) case, in which the fluids effects are not considered.

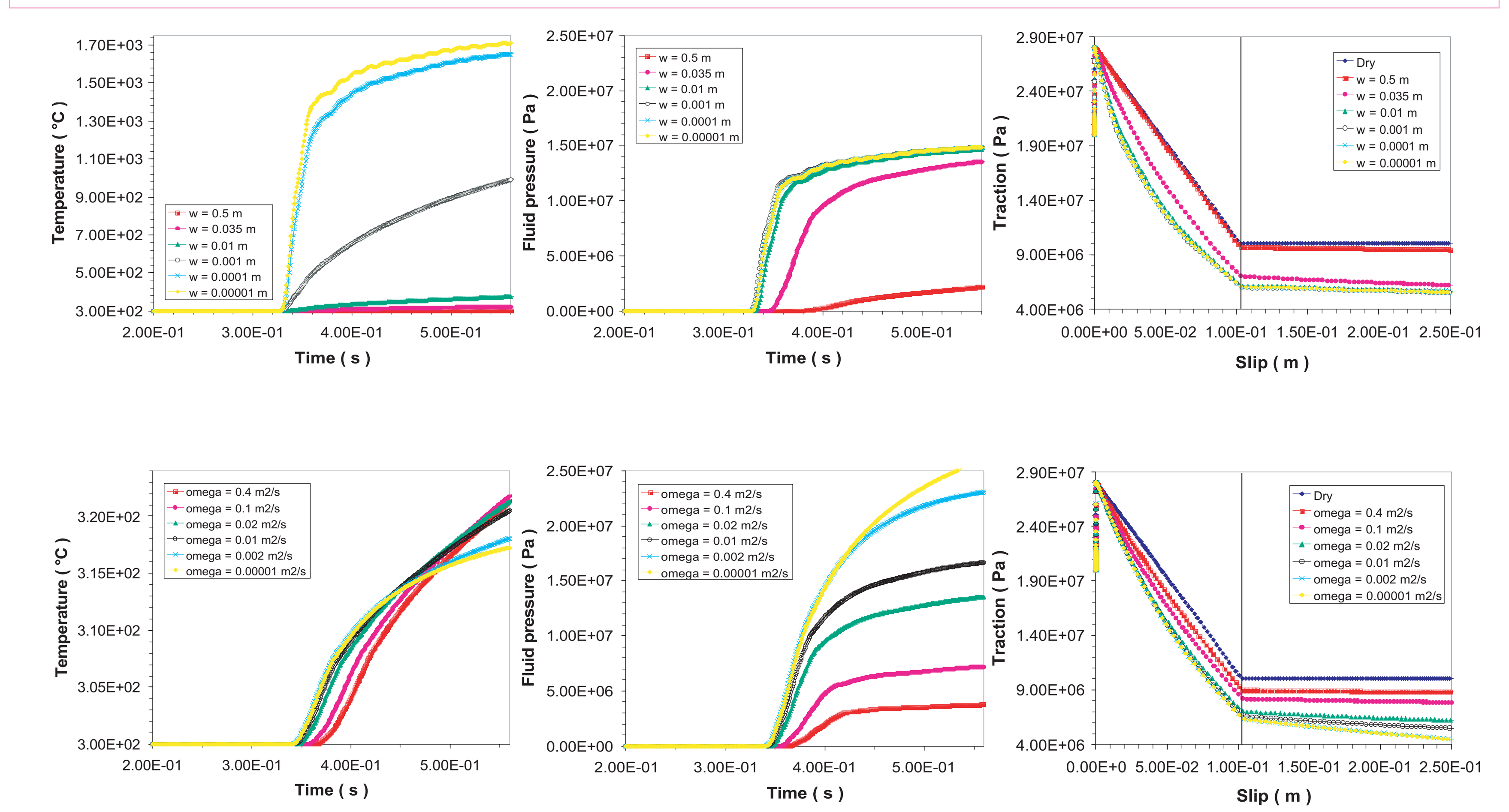

Figure 3

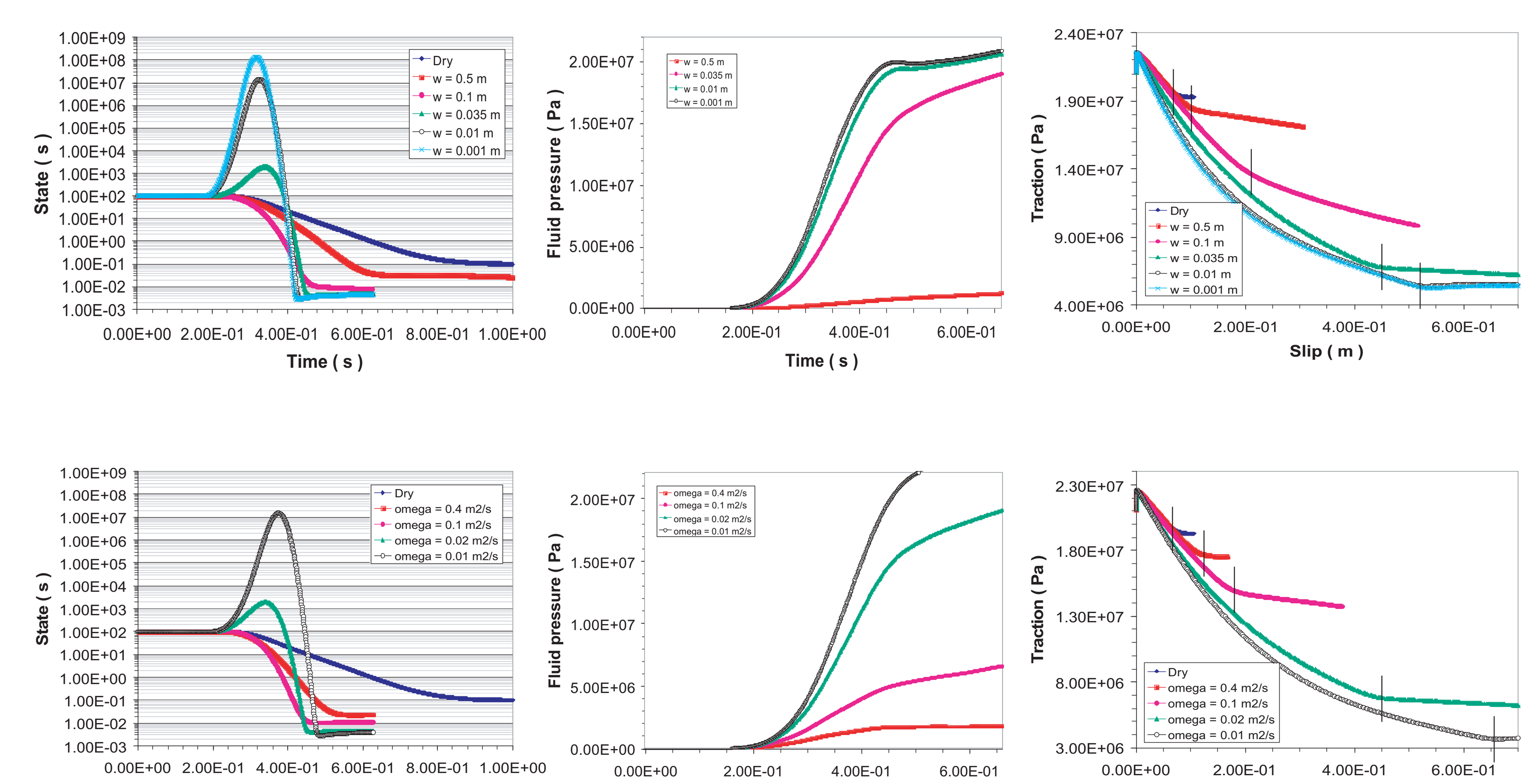

Figure 4

Dieterich-Ruina vs. Ruina-Dieterich

In Figure 5 we compare the results obtained with numerical experiment adopting the Dieterich-Ruina (DR, see Panel A) and the Ruina-Dieterich (RD) law, which for varying normal stress has the following form:

$$\tau=\left[\mu_*+a\,ln\left(\frac{v}{v_*}\right)+b\,ln\left(\frac{\Psi v_*}{L}\right)\right]\sigma_n^{eff}$$

$$\frac{\mathrm{d}}{\mathrm{d}t}\Psi=-\frac{\Psi v}{L}ln\left(\frac{\Psi v}{L}\right)-\left(\frac{\alpha_{LD}\Psi}{b\sigma_n^{eff}}\right)\frac{\mathrm{d}}{\mathrm{d}t}\sigma_n^{eff}$$

We can observe that even if the phase portraits are very similar, the traction evolution (in time and in slip) is quite different: this is due to the effect of variable normal stress that affects the state variable in the two models. In particular, the RD evolution equation does not admit the increase of the state variable and this cause an abrupt failure. As previously observed for Dry faults (Bizzarri and Cocco, 2003, *JGR, 108*), also in Wet conditions the state reaches a new steady state configuration. Moreover, in the RD case we can not define an equivalent characteristic SW distance, as the traction degrades like an exponential.

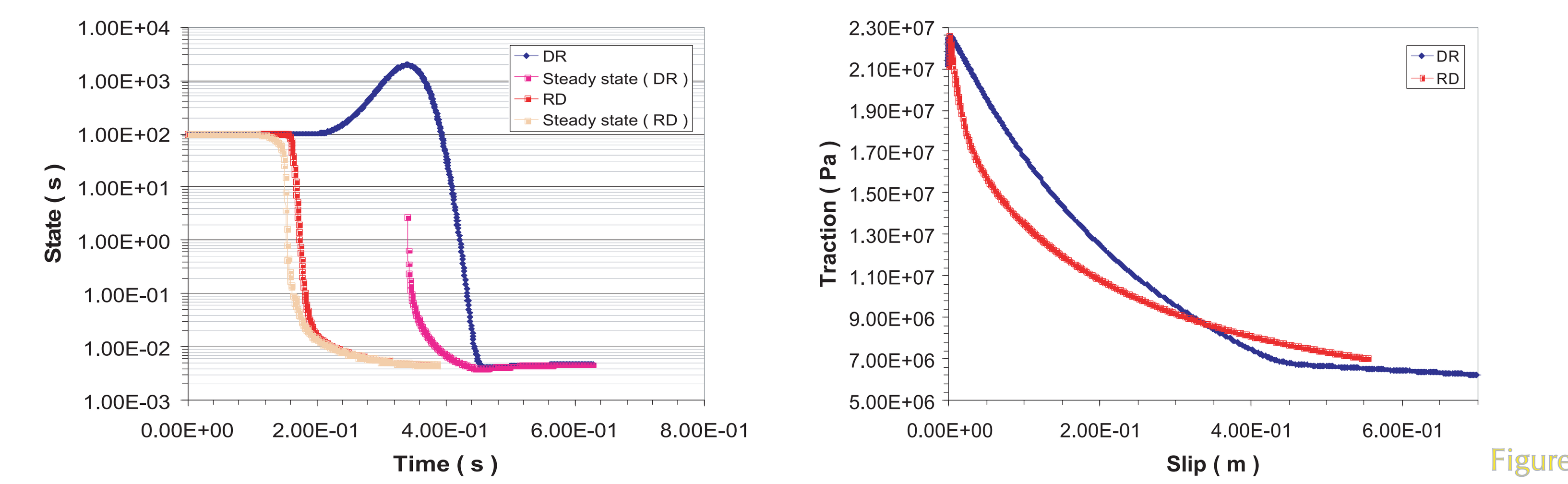

Figure 5

Variable Porosity

If the porosity Φ is not constant over the dynamic process, the generalized solution for the thermal pressurization problem is:

$$\tilde{p}_{fluid}^{\ wf}(\xi_1,\xi_2,t)=p_{fluid_0}^{\ f}+\frac{\gamma}{2w(\xi_1,\xi_2)}\int_0^{t-\varepsilon}\mathrm{d}t'\left\{-\frac{\chi}{\omega-\chi}\mathrm{erf}\left(\frac{w(\xi_1,\xi_2)}{2\sqrt{\chi(t-t')}}\right)+\frac{\omega}{\omega-\chi}\mathrm{erf}\left(\frac{w(\xi_1,\xi_2)}{2\sqrt{\omega(t-t')}}\right)\right\}$$

$$\left\{\tau(\xi_1,\xi_2,t')v(\xi_1,\xi_2,t')-\frac{2w(\xi_1,\xi_2)}{\gamma}\frac{1}{\beta_{fluid}\Phi(t')}\frac{\partial}{\partial t'}\Phi(t')\right\}$$

In Figure 6 we plot the results for a case in which the porosity evolution is expressed as (Segall and Rice, 1995):

$$\phi(t)=\phi_*-\varepsilon_{SR}\ln\left(\frac{\Psi v_*}{L_{SR}}\right)$$

assuming for simplicity that $L_{SR} = L$.

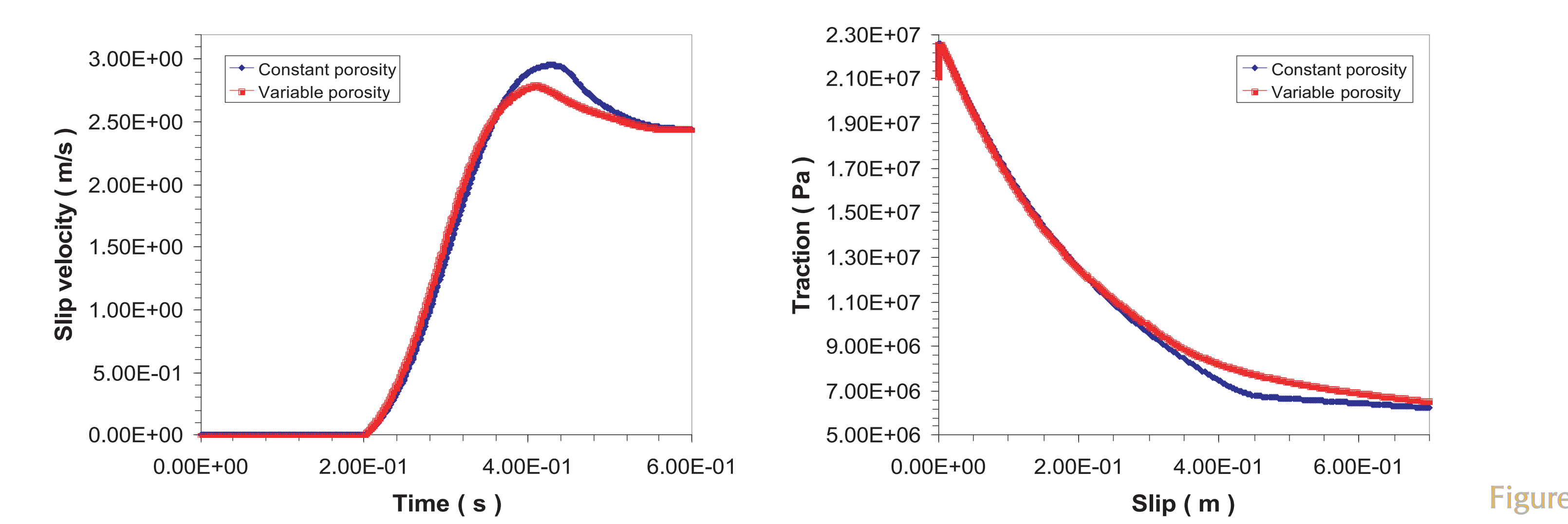

Figure 6

Conclusions

In this work we have made the following goals:

1) Thermal pressurization modifies the shape of the rupture front (see Figure 1 and Figure 2);

2) The breakdown stress drop (τ_u - τ_f) increases for decreasing values of the slip zone thickness $2w$ and hydraulic diffusivity ω;

3) Both w and ω affect the weakening rate;

4) The equivalent characteristic slip-weakening distance d_0^{eq} increases for decreasing w and ω;

5) Fluid pressure and normal stress variations modify the state variable evolution;

6) Evolution law does matter (see Figure 5);

7) Variable porosity makes impossible to identify d_0^{eq} and τ_f^{eq} (see Figure 6);

8) Healing and short slip durations with thermal pressurization reduces the *final* temperature increase due to fault slip, while the *instantaneous* temperature increase is similar to a crack like solutions;

9) In *Dry conditions*, for 60 cm of total fault slip, we obtain thermal variations from 35 °C (w=35 mm) to 1000 °C (w = 10 μm). In *Wet conditions*, for 1 m of total fault slip thermal variations are from 32 °C (w=35 mm) to 850 °C (w = 10 μm). Therefore we demonstrate that thermal pressurization may partially explain the heat flux paradox, as proposed by Sibson (1973, *Nature, 243*; 2003, *BSSA, 93*).